# Synthesis, Characterization, and Crystal Structures of a Series of Osmium−Rhodium Mixed-Metal Carbonyl Clusters: $[N(PPh_3)_2][Os_6Rh(\mu\text{-}H)_2(CO)_{20}]$, $[Os_6Rh(\mu\text{-}H)_7(\mu\text{-}CO)(CO)_{18}]$, $[Os_6Rh(\mu\text{-}H)_9(CO)_{18}]$, and $[Os_3Rh(\mu\text{-}CO)(CO)_9(\mu_4\text{-}\eta^2\text{-}PhC_2Ph)(\mu_2\text{-}\eta^1{:}\eta^2\text{-}PhC_2PhH)]$

Wing-Tak Wong

*Department of Chemistry, The University of Hong Kong, Pokfulam Road,*
*Hong Kong, People's Republic of China*

*Received February 12, 1999*

The reaction between $[N(PPh_3)_2][Os_3(\mu\text{-}H)(CO)_{11}]$ and $[Rh(COD)_2][SbF_6]$ (COD = cycloocta-1,5-diene) yields the known cluster $[Os_3Rh(\mu\text{-}H)_3(CO)_{10}(COD)]$ (**1**) and the new complex $[N(PPh_3)_2][Os_6Rh(\mu\text{-}H)_2(CO)_{20}]$ (**2**). Subsequent reaction of **1** with CO gas in $CH_2Cl_2$ produces $[Os_3Rh(\mu\text{-}H)_3(CO)_{12}]$ (**4**). Compound **1** also reacts with 1 equiv of $[N(PPh_3)_2][Os_3(\mu\text{-}H)(CO)_{11}]$ to give **2**. Hydrogenation of **1** results in the hydrogen-rich cluster $[Os_6Rh(\mu\text{-}H)_9(CO)_{18}]$ (**5**) in moderate yield. Reaction of **1** with diphenylacetylene affords $[Os_3Rh(\mu\text{-}CO)(CO)_9(\mu_4\text{-}\eta^2\text{-}PhC_2Ph)(\mu_2\text{-}\eta^1{:}\eta^2\text{-}PhC_2PhH)]$ (**6**). On the other hand, the unsaturated cluster $[Os_3(\mu\text{-}H)_2(CO)_{10}]$ reacts with $[Rh(dppm)_2][BF_4]$ (dppm = bis(diphenylphosphino)methane) to give $[Os_6Rh(\mu\text{-}H)_7(\mu\text{-}CO)(CO)_{18}]$ (**3**) in good yield. The crystal structures of **2**, **3**, **5**, and **6** were determined. Clusters, **2**, **3,** and **5** consist of a central rhodium atom linking two triosmium units; however, the rhodium atom of **2** bridges two triosmium units, while **3** and **5** possess a sandwich-type structure. Complex **6** has a butterfly arrangement of three osmium atoms and one rhodium atom which contains a diphenylacetylene fragment in a $\mu_4\text{-}\eta^2$ arrangement and an alkenyl group in a $\mu_2\text{-}\eta^1{:}\eta^2$ configuration.

## Introduction

Heterometallic cluster compounds have received considerable attention because of their potential for novel catalytic and stoichiometric reactions.[1,2] The arrangement of metal atoms on the surface of these clusters sometimes resembles the arrangement on the surface of bulk metals. Both osmium and rhodium are susceptible to the formation of large metal carbonyl clusters,[3−9] and so we are interested in osmium−rhodium carbonyl systems.

Recently, we reported the synthesis of two novel high-nuclearity clusters, $[Os_{12}Rh_9(CO)_{44}(\mu_3\text{-}Cl)]$ and $[Os_4Rh_3(\mu_3\text{-}H)(CO)_{14}(\eta^4\text{-}C_7H_8)_2]$, via a redox condensation reaction.[10] The current paper describes the coupling reaction of $[Os_3(\mu\text{-}H)(CO)_{11}]^-$ with $[Rh(COD)_2]^+$ (COD = cycloocta-1,5-diene) and the reaction of $[Os_3(\mu\text{-}H)_2(CO)_{10}]$ with $[Rh(dppm)_2]^+$ leading to heptanuclear mixed-metal clusters.

The displacement of weakly coordinating ligands, such as COD, by a strong π base or metal nucleophile is now a relatively common approach to cluster synthesis. It offers the advantages of mild reaction conditions and control of stoichiometry in the cluster-forming reaction. Stone and co-workers developed this approach, using $[Pt(COD)_2]$ and related compounds as a source of $Pt^0$ to prepare several heteronuclear clusters containing platinum.[11] The reactions of $[Os_3Rh(\mu\text{-}H)_3(CO)_{10}(COD)]$ (**1**) with small molecules, including carbon monoxide, hydrogen, and diphenylacetylene were also studied.

## Results and Discussion

**Synthesis of $[Os_3Rh(\mu\text{-}H)_3(CO)_{10}(COD)]$ (1) and $[N(PPh_3)_2][Os_6Rh(\mu\text{-}H)_2(CO)_{20}]$ (2).** When the anionic triosmium cluster $[Os_3(\mu\text{-}H)(CO)_{11}]$ was allowed to react with a stoichiometric amount of $[Rh(COD)_2]^+$ cation at room temperature, the known cluster $[Os_3Rh(\mu\text{-}H)_3(CO)_{10}(COD)]$[12] (**1**) was identified as the major product by IR, $^1H$ NMR, and MS (Scheme 1). A minor product, $[Os_6Rh(\mu\text{-}H)_2(CO)_{20}]^-$, was also isolated as its $[N(PPh_3)_2]^+$ salt (**2**) and was characterized by various

---

[1] Adams, R. D., Cotton, F. A., Eds. *Catalysis by Di- and Polynuclear Metal Cluster Complexes*; Wiley-VCH: New York, 1998.

[2] Nashner, M. S.; Somerville, D. M.; Lane, P. D.; Adler, D. L.; Shapley, J. R.; Nuzzo, R. G. *J. Am. Chem. Soc.* **1996**, *118*, 12964.

[3] Amoroso, A. J.; Johnson, B. F. G.; Lewis, J.; Raithby, P. R.; Wong, W. T. *J. Chem. Soc., Chem. Commun.* **1991**, 814.

[4] Amoroso, A. J.; Johnson, B. F. G.; Lewis, J.; Raithby, P. R.; Wong, W. T. *Angew. Chem., Int. Ed. Engl.* **1991**, *30*, 1505.

[5] Braga, D.; Lewis, J.; Johnson, B. F. G.; McPartlin, M.; Nelson, W. J. H.; Vargas, M. D. *J. Chem. Soc., Chem. Commun.* **1983**, 241.

[6] Braga, D.; Henrick, K.; Johnson, B. F. G.; Lewis, J.; McPartlin, M.; Nelson, W. J. H.; Vargas, M. D. *J. Chem. Soc., Chem. Commun.* **1982**, 419.

[7] Ciani, G.; Moret, M.; Fumagalli, A.; Martinengo, S. *Inorg. Chem.* **1989**, *28*, 2011.

[8] Vidal, J. L; Fiato, R. A.; Cosby, L. A.; Pruett, R. L. *Inorg. Chem.* **1978**, *17*, 2574.

[9] Vidal, J. L; Walker, W. E.; Pruett, R. L.; Schoening, R. C. *Inorg. Chem.* **1979**, *18*, 129.

[10] Hung, S. Y. W.; Wong, W. T. *J. Chem. Soc., Chem. Commun.* **1997**, 2099.

[11] Stone, F. G. A. *Inorg. Chim. Acta* **1981**, *50*, 33.

[12] Sundberg, P.; Noren, B.; Johnson, B. F. G.; Lewis, J.; Raithby, P. R. *J. Organomet. Chem.* **1988**, *353*, 383.

10.1021/om9900925 CCC: $18.00
Publication on Web 07/28/1999

**Scheme 1**[a]

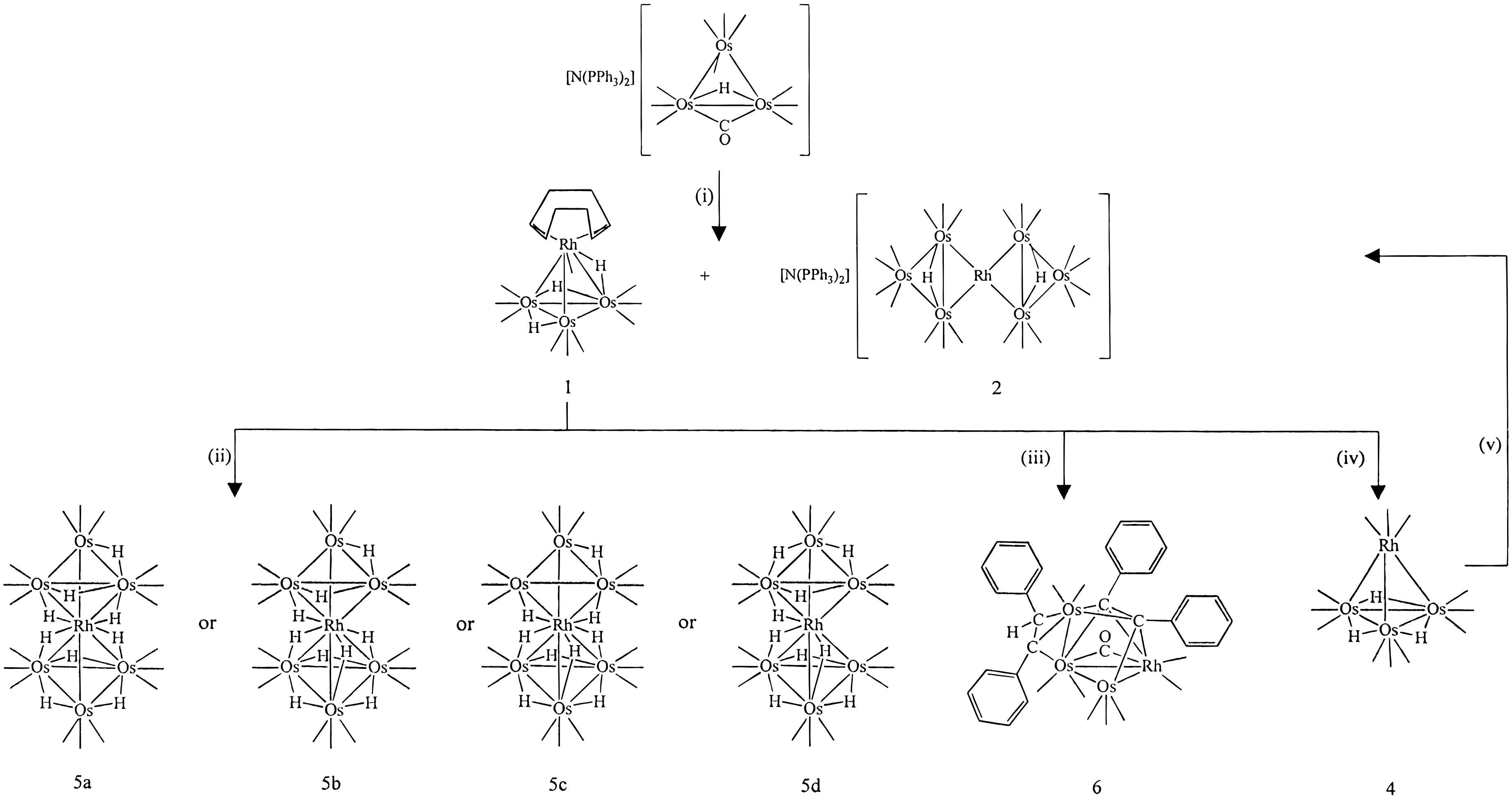

[a] Legend: (i) $[Rh(COD)_2][SbF_6]$, $CH_2Cl_2$; (ii) $H_2$, $CH_2Cl_2$; (iii) $PhC_2Ph$, refluxing $CHCl_3$; (iv) $CO/CH_2Cl_2$; (v) $[N(PPh_3)][Os_3(\mu\text{-}H)(CO)_{12}]/CH_2Cl_2$.

**Table 1. Spectroscopic Data for Complexes 2, 3, 5, and 6**

| compd | IR spectra[a] ($\nu$(CO)/cm$^{-1}$) | mass spectra[b] ($m/z$) | $^1$H NMR spectra[c] ($\delta$) |
|---|---|---|---|
| **2** | 2076 m, 2040 s, 1987 s, 1952 sh | 1807 (1807) | −12.65 [s, 2H, OsHOs] |
| **3** | 2118 w, 2097 m, 2082 s, 2064 s, 2043 w, 2018 m, 2010 m, 1997 w, 1740 w | 1784 (1784) | at 25 °C: −19.54 [m, br, 7H] |
| | | | at −50 °C: −17.51 [m, br, 1H], −18.10 [m, br, 1H], −18.79 [m, br, 1H], −19.37 [m, br, 2H], −20.90 [m, br, 1H], −23.42 [m, br, 1H] |
| **5** | 2086 m, 2065 s, 2041 s, 2017 s, 1981w | 1758 (1758) | at 25 °C: −19.45 [m, br, 5H], −19.73 [m, br, 4H] |
| | | | at −50 °C: −17.43 [m, br, 1H], −18.13 [m, br, 1H], −18.67 [m, br, 1H], −19.34 [m, br, 3H], −20.30 [m, br, 1H], −20.95 [m, br, 1H], −23.49 [m, br, 1H] |
| **6** | 2130 w, 2080 s, 2064 m, 2055 s, 2045 s, 2033 s, 2022 m, 2008 s, 1997 m, 1987 sh, 1966 m, 1948 w, 1752 w | 1311 (1311) | 7.21 [m, 20H, aryl H], 4.03 [s, br, 1H, alkenyl H] |

[a] Recorded in *n*-hexane except for **2**, which was recorded in $CH_2Cl_2$. [b] +ve FAB for **3**, **5**, and **6**, −ve FAB for **2**; simulated values in parentheses. [c] Recorded in $CD_2Cl_2$.

**Table 2. Selected Bond Distances (Å) and Angles (deg) for Cluster 2[a]**

| | | | |
|---|---|---|---|
| Os(1)−Os(2) | 2.669(1) [2.676(1)] | Os(1)−Os(3) | 2.840(1) [2.828(1)] |
| Os(2)−Os(3) | 2.829(1) [2.833(1)] | Os(1)−Rh(1) | 2.8680(8) [2.8531(8)] |
| Os(2)−Rh(1) | 2.8771(8) [2.8686(7)] | Os(1)−C(1) | 1.85(3) [1.85(2)] |
| Os(1)−C(2) | 1.77(2) [1.83(2)] | Os(1)−C(3) | 1.84(3) [1.88(2)] |
| Os(2)−C(4) | 1.84(2) [1.84(2)] | Os(3)−C(7) | 1.90(2) [1.88)(2)] |
| P(1)−N(1) | 1.560(7) [1.570(7)] | P(1)−C(21) | 1.79(2) [1.79(2)] |
| Os(1)−Os(3)-Os(2) | 56.17(3) [56.42(3)] | Os(2)−Os(1)−Rh(1) | 62.49(2) [62.41(2)] |
| Os(3)−Os(1)−Rh(1) | 96.62(3) [96.35(3)] | Os(1)−Os(2)−Rh(1) | 62.15(2) [61.82(2)] |
| Os(3)−Os(2)−Rh(1) | 96.66(3) [95.89(3)] | Os(1)−Rh(1)−Os(2) | 55.36(2) [55.77(2)] |
| Os(1)−Rh(1)-Os(2*) | 124.64(2) [124.23(2)] | | |

[a] Values for the second molecule are given in brackets.

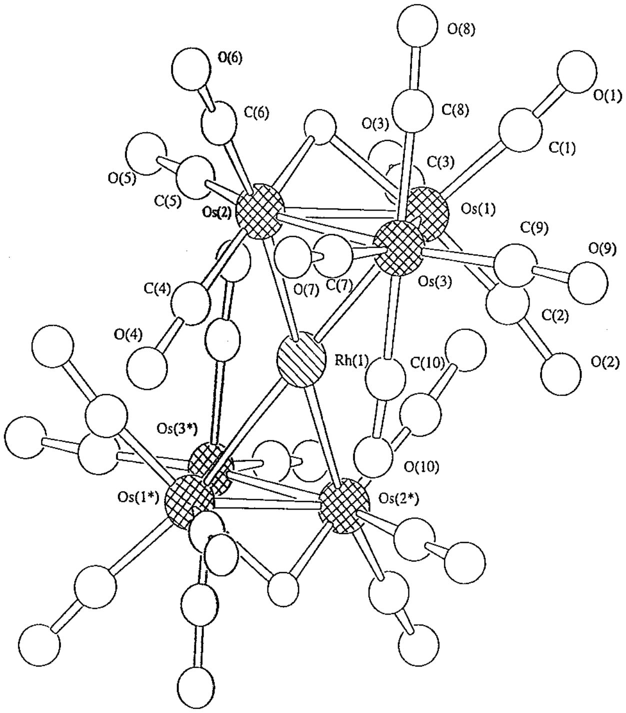

**Figure 1.** Molecular structure of cluster **2** showing the atomic numbering scheme for non-hydrogen atoms.

spectroscopic methods (Table 1). The negative FAB mass spectrum exhibited an envelope centered at $m/z$ 1807 with an isotopic distribution of six osmium atoms and one rhodium atom. The $^1$H NMR spectrum recorded at room temperature shows a sharp singlet centered at $\delta$ −12.65 ppm, which is attributed to the two hydride ligands bridging equivalent Os−Os edges. This singlet remains at −50 °C. There were no NMR signals detected that indicated the presence of COD in complex **2**. The IR spectrum showed the presence of only terminal carbonyl ligands in solution. To elucidate the structure of cluster **2**, an X-ray analysis was carried out on a dark green crystal grown by slow evaporation of a *n*-hexane/dichloromethane solution at 10 °C. There are two independent but similar half-molecules in an asymmetric unit. Each molecule contains the cluster anion and the counterion $[N(PPh_3)_2]^+$.

The crystal structure of the anionic part $[Os_6Rh(\mu\text{-}H)_2(CO)_{20}]^-$ is depicted in Figure 1, and relevant structural parameters are given in Table 2. Complex **2** is essentially isostructural with $[N(PPh_3)_2][Os_6Au(\mu\text{-}H)_2(CO)_{20}]$.[13] The molecule consists of two $Os_3$ cluster units linked by a "naked" rhodium atom with $C_{2h}$ point symmetry for the molecule. The metal framework may also be described as two butterfly fragments sharing a common wing-tip vertex. The hydrides of **2** are inferred to bridge across Os(1)−Os(2) and the symmetry-related Os(1*)−Os(2*). This is evident from the $^1$H NMR spectrum, which consists of a singlet and therefore indicates no H−Rh interaction. The structure of each $\{Os_3(\mu\text{-}H)(CO)_{10}\}$ unit in **2** is closely related to that of $[Os_3(\mu\text{-}H)_2(CO)_{10}]$.[15] Both of these are electronically unsaturated, with only 46 cluster valence electrons (CVE). The Os(1)−Os(2) bond (2.669(1) Å) is doubly bridged by hydride ligands and a rhodium atom. This observed distance is comparable to that in $[Os_3(\mu\text{-}H)_2(CO)_{10}]$, where the presence of a multiple metal−metal bond is suggested.[14] The average Os−Rh bond distance of **2** is found to be 2.8726(8) Å, which is significantly longer than for such bonds in the tetrahedral cluster $[Os_3Rh(\mu\text{-}H)_3(CO)_{12}]$[12] (average Os−Rh 2.763 Å). The arrangement around the Rh(1) atom of **2** is square

---

(13) Johnson, B. F. G.; Kaner, D. A.; Lewis, J.; Raithby, P. R. *J. Chem. Soc., Chem. Commun.* **1981**, 753.

(14) Orpen, A. G.; Rivera, A. V.; Bryan, E. G.; Pippard, D.; Sheldrick, G. M.; Rouse, K. D. *J. Chem. Soc., Chem. Commun.* **1978**, 723.

(15) Broach, R. W.; Williams, J. M. *Inorg. Chem.* **1979**, *18*, 314.

**Scheme 2**[a]

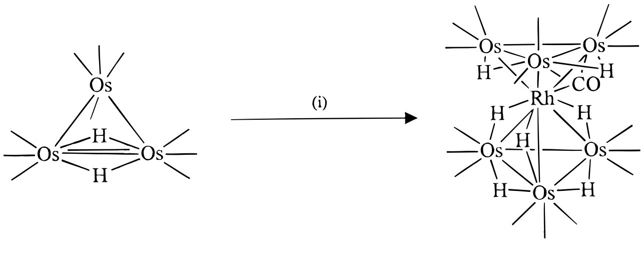

**3**

[a] Legend: (i) $[Rh(dppm)_2][BF_4]$, refluxed in $CHCl_3$.

planar, as is the case for the central metal atom in the related mixed-metal cluster $[Fe_4Pd(CO)_{16}]^{2-}$.[16] In compound **2** the Rh atom adopts a stable 16-electron configuration.

**Synthesis of $[Os_6Rh(\mu\text{-}H)_7(\mu\text{-}CO)(CO)_{18}]$ (3).** Treatment of the air-sensitive compound $[Rh(dppm)_2][BF_4]$ with 1 equiv of $[Os_3(\mu\text{-}H)_2(CO)_{10}]$ gave $[Os_6Rh(\mu\text{-}H)_7(\mu\text{-}CO)(CO)_{18}]$ (**3**) (Scheme 2), which was isolated as a red solid after TLC separation. This new red complex was fully characterized by IR, $^1H$ NMR, and mass spectroscopy (Table 1). Its mass spectrum exhibited a molecular ion peak at $m/z$ 1784. The variable-temperature $^1H$ NMR spectrum in the range of $\delta$ −10 to −30 ppm indicated the occurrence of fluxional processes associated with the hydride ligands. A complex pattern at $\delta$ −19.54 ppm was split into six broad multiplet signals in the range $\delta$ −17.51 to −23.42 ppm in the ratio 1:1:1:2:1:1 at −50 °C. These observed complex multiplets are due to the combined effect of $^1H-^1H$ coupling between nonequivalent hydrides and $^1H-Rh$ coupling. Although the signals are not well-resolved, complex **3** is thought to contain seven chemically nonequivalent metal hydrides. In the infrared spectrum of **3**, a small hump at 1740 $cm^{-1}$ is attributed to a bridging carbonyl.

A single-crystal X-ray diffraction study was undertaken on the red rod-shaped crystals of complex **3**. A perspective view of **3** is depicted in Figure 2 with some interatomic distances and angles tabulated in Table 3. The compound crystallizes in the monoclinic space group $P2_1/n$. The cluster can be described as the combination of two $\{Os_3Rh\}$ tetrahedra which share a common rhodium vertex. A similar "sandwich-type" metal skeleton has been observed in $[Hg\{Pt_3(2,6\text{-}Me_2C_6H_3NC)_6\}]$[17] and $[M\{Pt(\mu\text{-}CO)_3L_3\}_2]^+$ (M = Cu,[18] Ag,[19] and Au;[20] L = tertiary phosphine). The dihedral angle between the two osmium triangles of **3** is 159.07°; consequently, they are arranged in an approximately eclipsed conformation. Of the six mixed-metal bonds found in the structure, two (Os(5)–Rh(1) and Os(6)–Rh(1)) are unsupported, with an average bond distance of 2.764(1) Å; the Os(4)–Rh(1) edge is asymmetrically bridged by a carbonyl ligand (Os(4)–C(19) = 2.28(1) Å, Rh(1)–C(19) = 1.90(1) Å), while the longest bonds, Os(1)–Rh(1) (2.941(1) Å), Os(2)–Rh(1) (2.947(1) Å), and Os(3)–Rh(1) (2.923(1) Å) are each singly bridged by a metal hydride. The osmium–osmium bond lengths range from 2.8092(7) to 3.0307(7) Å, and hydride ligands are thought to bridge Os(1)–Os(2), Os(1)–Os(3), Os(4)–Os(5), and Os(5)–Os(6), which are the longest edges (2.9188(7)–3.0307(7) Å). There are three terminally coordinated carbonyls to each osmium metal so the proposed structure obeys the EAN rule with 102 CVE, where the Rh atom assumes an 18-electron configuration. However, this formulation is based on the poorly resolved low-temperature NMR work. One cannot rule out the possibility that only five hydrides are present, in which case the Rh atom would adopt a 16-electron configuration.

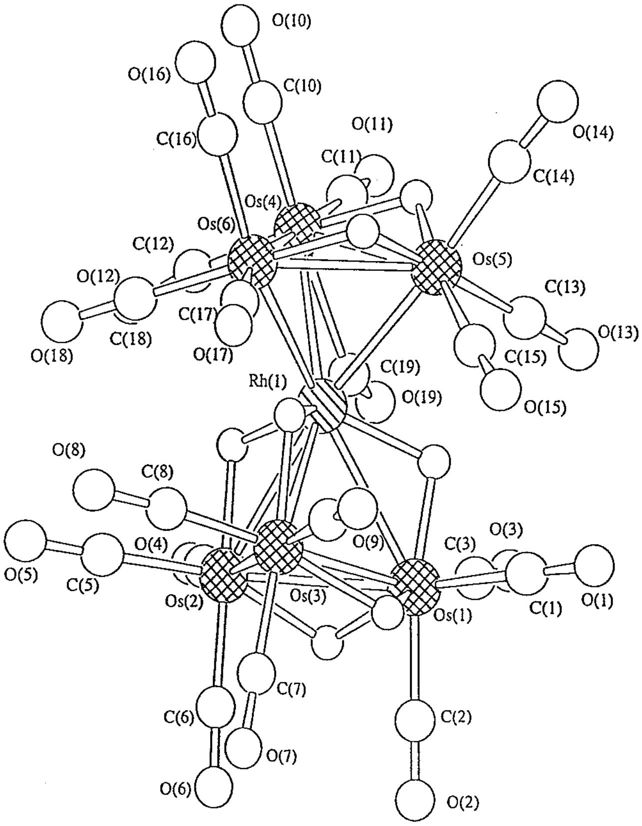

**Figure 2.** Molecular structure of cluster **3** showing the atomic numbering scheme for non-hydrogen atoms.

**Table 3. Selected Bond Distances (Å) and Angles (deg) for Cluster 3**

| | | | |
|---|---|---|---|
| Os(1)–Os(2) | 3.0307(7) | Os(1)–Os(3) | 2.9870(7) |
| Os(2)–Os(3) | 2.8092(7) | Os(4)–Os(5) | 2.9254(7) |
| Os(4)–Os(6) | 2.8295(7) | Os(5)–Os(6) | 2.9188(7) |
| Os(1)–Rh(1) | 2.941(1) | Os(2)–Rh(1) | 2.947(1) |
| Os(3)–Rh(1) | 2.923(1) | Os(4)–Rh(1) | 2.758(1) |
| Os(5)–Rh(1) | 2.750(1) | Os(6)–Rh(1) | 2.777(1) |
| Os(4)–C(19) | 2.28(1) | Rh(1)–C(19) | 1.90(1) |
| O(19)–C(19) | 1.17(1) | | |
| Os(2)–Os(1)–Os(3) | 55.65(2) | Os(1)–Os(2)–Os(3) | 61.39(2) |
| Os(1)–Os(3)–Os(2) | 62.96(2) | Os(5)–Os(4)–Os(6) | 60.93(2) |
| Os(4)–Os(5)–Os(6) | 57.91(2) | Os(4)–Os(6)–Os(5) | 61.16(2) |
| Os(1)–Rh(1)–Os(2) | 61.96(2) | Os(1)–Rh(1)–Os(3) | 61.24(2) |
| Os(2)–Rh(1)–Os(3) | 57.18(2) | Os(4)–Rh(1)–Os(5) | 64.17(3) |
| Os(4)–Rh(1)–Os(6) | 61.48(3) | Os(5)–Rh(1)–Os(6) | 63.75(3) |

**Reactivity of $[Os_3Rh(\mu\text{-}H)_3(CO)_{10}(COD)]$ (1).** Cluster **1** can be obtained by two other synthetic means: (i) the substitution reaction of $[Os_3Rh(\mu\text{-}H)_3(CO)_{12}]$ (**4**) with an excess of COD in the presence of $Me_3NO$[13] and (ii) treatment of $[Os_3(\mu\text{-}H)_2(CO)_{10}]$ with 1 equiv of [Rh-

---

(16) Longoni, G.; Manassero, M.; Sansoni, M. *J. Am. Chem. Soc.* **1980**, *102*, 3242.

(17) Dahmen, K. H. Ph.D. Thesis, ETH Zurich N, 1986.

(18) Yamamoto, Y.; Yamazaki, H.; Sakurai, T. *J. Am. Chem. Soc.* **1982**, *104*, 2329.

(19) Albinati, A.; Dahmen, K. H.; Togni, A.; Venanzi, L. M. *Angew. Chem., Int. Ed. Engl.* **1985**, *97*, 760.

(20) Hallam, M. F.; Mingos, D. M. P.; Adatia, T.; McPartlin, M. *J. Chem. Soc., Dalton Trans.* **1987**, 335.

(COD)(N)I] (N = 2,2′-bipyridine, 1,10-phenanthroline, and 4,4′-diphenyl-2,2′-bipyridine) in refluxing dichloromethane.[21] The formation of **1** in good yield by several synthetic routes offered us the opportunity to study its reactivity.

**Carbonylation.** The carbonylation reaction of **1** under room conditions has been found to give [$Os_3Rh(\mu\text{-}H)_3(CO)_{12}$] (**4**) in good yield as the sole product. The crystal structure of **4** has previously been reported by Lewis and co-workers.[12]

**Hydrogenation.** Cluster **1** was hydrogenated (1 atm, 25 °C) in dichloromethane for 15 h to give the major product [$Os_6Rh(\mu\text{-}H)_9(CO)_{18}$] (**5**) (Scheme 1). The solution IR spectrum (Table 1) of **5** showed only terminal carbonyl stretching frequencies. The positive FAB mass spectrum exhibited a parent envelope centered at $m/z$ 1758. The absence of COD in **5** was indicated by $^1H$ NMR spectroscopy. There are two broad multiplets at $\delta$ −19.45 and −19.73 ppm with an integral ratio of 5:4. These broad signals are presumably caused by rapid intramolecular exchange of the hydride ligands in solution state at room temperature, which is similar to the case of complex **3**. As the temperature is decreased to −50 °C, these broad peaks of hydride signals turned into seven broad multiplets in the ratio 1:1:1:3:1:1:1 ranging from $\delta$ −17.0 to −24.0 ppm. We cannot construct any static model of **5** to explain the observed integral ratio for the hydrides at this temperature. One possibility is that all hydrides are bridging different metal−metal edges so that the limiting $^1H$ NMR spectrum should contain nine signals for hydrides with equal intensity, but some of these signals overlap to give the observed pattern. Some suggested models are shown in Scheme 1. However, the solubility and resolution problems associated with the $^1H$ NMR studies preclude unambiguous assignments for these hydride ligands.

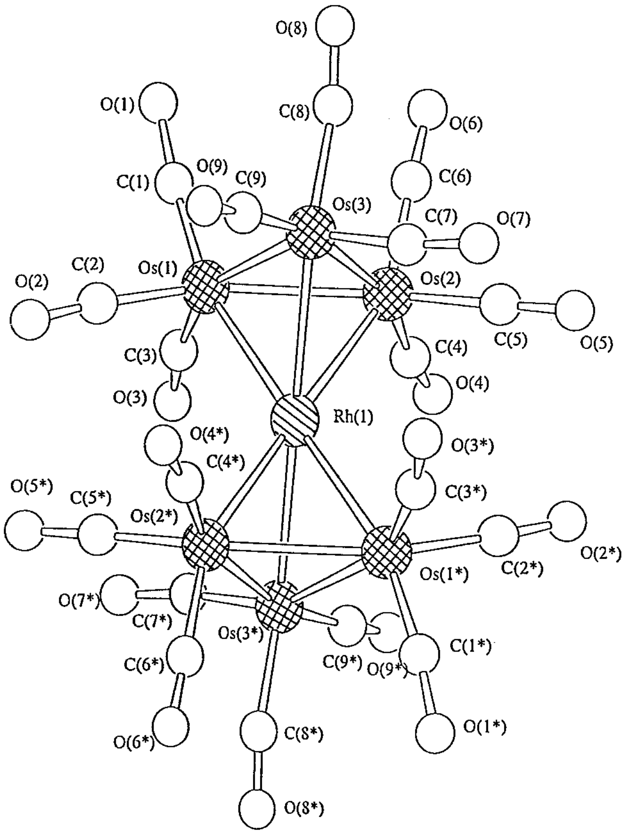

**Figure 3.** Molecular structure of cluster **5** showing the atomic numbering scheme for non-hydrogen atoms.

**Table 4. Selected Bond Distances (Å) and Angles (deg) for Cluster 5**

| | | | |
|---|---|---|---|
| Os(1)−Os(2) | 2.932(1) | Os(1)−Os(3) | 2.967(1) |
| Os(2)−Os(3) | 2.847(2) | Os(1)−Rh(1) | 2.8769(8) |
| Os(2)−Rh(1) | 2.892(1) | Os(3)−Rh(1) | 2.858(1) |
| Os(2)−Os(1)-Os(3) | 57.72(3) | Os(1)−Os(2)−Os(3) | 61.76(3) |
| Os(1)−Os(3)−Os(2) | 60.53(3) | Os(2)−Os(1)−Rh(1) | 59.70(3) |
| Os(1)−Os(2)−Rh(1) | 59.21(2) | Os(3)−Os(2)−Rh(1) | 59.74(3) |
| Os(1)−Rh(1)−Os(2) | 61.09(3) | Os(1)−Rh(1)−Os(2) | 118.91(3) |
| Os(1)−Rh(1)−Os(2*) | 118.91(3) | Os(1)−Rh(1)−Os(3*) | 117.70(3) |
| Os(2)−Rh(1)−Os(3*) | 120.64(3) | | |

To elucidate the structure of **5**, an X-ray analysis was carried out on the red crystals of the complex, formed by slow evaporation of a saturated $CH_2Cl_2$/$n$-hexane solution for a period of 2 days. The molecular structure is illustrated in Figure 3, and selected bond parameters are presented in Table 4. Compound **5** shows a metal disposition like that of **3**, containing a vertex-shared (Rh(1)) bitetrahedron. The main structural difference between **5** and **3** is the replacement of a bridging hydride ligand by a bridging carbonyl ligand. In addition, the $Os_3$ triangles in **5** are parallel and exactly staggered, while those in **3** are not. The platinum [$Os_6Pt(\mu\text{-}H)_8(CO)_{18}$][22] and palladium [$Os_6Pd(\mu\text{-}H)_8(CO)_{18}$][23] analogues of **5** have been synthesized by the hydrogenation of [$Os_4Pt_2(CO)_{18}$] and the reaction of [$Os_3(\mu\text{-}H)_2(CO)_{10}$] with *trans*-[$Pd(NH_3)_2I_2$], respectively. Each osmium atom contains three linear terminal carbonyl ligands. The osmium−osmium bond distances, which range from 2.847(2) to 2.967(1) Å, compare well with the corresponding average value (2.926 Å) found in the cluster [$Os_6Pd(\mu\text{-}H)_8(CO)_{18}$]. The Os−Rh separations (2.858(1)−2.892(1) Å) are slightly greater than the corresponding mean value for [$Os_3Rh(\mu\text{-}H)_3(CO)_{12}$] (2.763 Å).[13] However, the crystal structure analysis of **5** does not allow the determination of hydride positions with certainty, because the rhodium atom coincides with the crystallographic inversion center, so that the two $Os_3$ triangles are related. This pseudo-symmetry problem precludes a detailed analysis of metal−metal bond distance due to the hydride bridging effect.

**Reaction of 1 with $PhC_2Ph$.** The reaction of [$Os_3Rh(\mu\text{-}H)_3(CO)_{10}(COD)$] (**1**) with diphenylacetylene ($PhC_2Ph$) at 60 °C led to the formation of [$Os_3Rh(\mu\text{-}CO)(CO)_9(\mu_4\text{-}\eta^2\text{-}PhC_2Ph)(\mu_2\text{-}\eta^2{:}\eta^1\text{-}PhC_2PhH)$] (**6**). However, no reaction was observed at room temperature. It is believed that the elevated temperature initiated the dissociation of the COD ligand from [$Os_3Rh(\mu\text{-}H)_3(CO)_{10}(COD)$] (**1**) and the subsequent addition of 2 equiv of $PhC_2Ph$ to form **6**. The product has been fully characterized by spectroscopic techniques, and these data are collected in Table 1. Microanalysis, supported by FAB mass spectra, indicated the formulation of [$Os_3Rh(H)(CO)_{10}(PhC_2Ph)_2$] for **6**. The infrared data of **6** in $n$-hexane shows an edge-bridging carbonyl absorption at 1752 cm$^{-1}$. A set of unresolved multiplets centered

---

[21] Hung, S. Y. W.; Wong, W. T. *J. Organomet. Chem.* **1998**, *566*, 237.

[22] Adams, R. D.; Pompeo, M. P.; Wu, W. *Inorg. Chem.* **1991**, *30*, 2425.

[23] Hui, J. W. S.; Wong, W. T. *J. Chem. Soc., Dalton Trans.* **1997**, 1515.

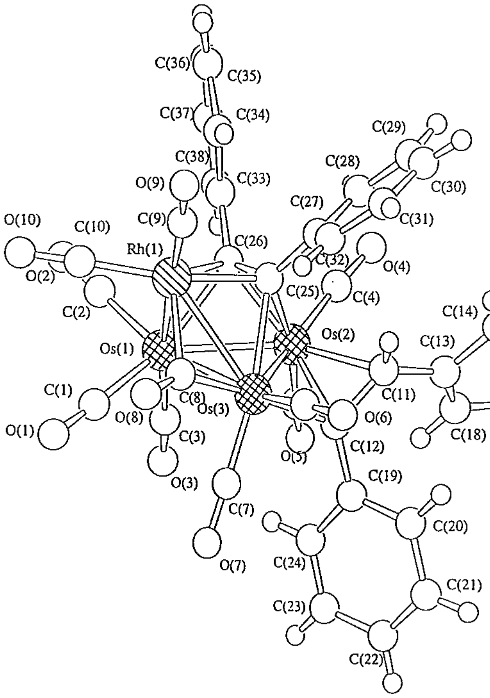

**Figure 4.** Molecular structure of cluster **6** showing the atomic numbering scheme for non-hydrogen atoms.

**Table 5. Selected Bond Distances (Å) and Angles (deg) for Cluster 6**

| | | | |
|---|---|---|---|
| Os(1)−Os(2) | 2.749(1) | Os(1)−Os(3) | 2.892(1) |
| Os(2)−Os(3) | 2.701(1) | Os(1)−Rh(1) | 2.694(2) |
| Os(3)−Rh(1) | 2.802(2) | Os(3)−Rh(1) | 2.802(2) |
| Os(1)−C(26) | 2.19(2) | Os(2)−C(25) | 2.28(2) |
| Os(2)−C(26) | 2.17(2) | Os(3)−C(8) | 2.06(2) |
| Os(3)−C(12) | 2.16(2) | Os(3)−C(25) | 2.28(2) |
| Rh(1)−C(8) | 2.10(2) | Rh(1)−C(25) | 2.19(2) |
| Rh(1)−C(26) | 2.34(2) | C(11)−C(12) | 1.43(3) |
| C(25)−C(26) | 1.48(3) | | |
| Os(2)−Os(1)−Os(3) | 57.16(3) | Os(1)−Os(2)−Os(3) | 64.10(3) |
| Os(1)−Os(3)−Os(2) | 58.74(3) | Os(2)−Os(1)−Rh(1) | 91.33(4) |
| Os(3)−Os(1)−Rh(1) | 60.08(4) | Os(1)−Os(3)−Rh(1) | 56.44(4) |
| Os(2)−Os(3)−Rh(1) | 90.03(4) | Os(1)−Rh(1)−Os(3) | 63.48(4) |

at $\delta$ 7.21 ppm and a broad signal at $\delta$ 4.03 ppm are observed in the $^1$H NMR spectrum, and they are assigned to the aryl protons and alkenyl proton, respectively.

To determine the precise ligand arrangement in **6**, a crystal structure determination was undertaken. The full structure as well as selected bond lengths and angles of **6** are shown in Figure 4 and Table 5, respectively. Complex **6** contains a butterfly metal framework of three osmium atoms and one rhodium atom, where the latter occupies one wing-tip site. A dihedral angle of 66.21° between the wings (Os(1)−Os(2)−Os(3) and Os(1)−Rh(1)−Os(3)) was determined. The hinge bond Os(1)−Os(3) (2.892(1) Å) is longer than the two wing edges (Os(1)−Os(2), 2.749(1) Å; Os(2)−Os(3), 2.701(1) Å), while the mixed-metal edge Os(1)−Rh(1) (2.694(2) Å) is shorter than Os(3)−Rh(1) (2.802(2) Å) by 0.108 Å. There is one diphenylacetylene ligand and one alkenyl ligand in the solid-state structure of complex **6**. The $Ph_2C_2$ ligand attaches to all metal atoms to form a distorted *closo*-$Os_3RhC_2$ octahedron with each acetylenic carbon atom forming one metal−carbon $\sigma$ bond to the two hinge atoms (Os(1) and Os(3)) of average length 2.24 Å and two $\pi$ bonds to the wing-tip atoms (Os(2) and Rh(1)) of average length 2.26 Å. The alkenyl group, $PhC_2PhH$, bridges the Os(2)−Os(3) edge of the metal core with C(11) bonded to Os(2) (2.23(2) Å) and C(12) linked to Os(2) (2.15(2) Å) and Os(3) (2.16(2) Å). The two C−C bonds (C(11)−C(12), 1.43(3) Å; C(25)−C(26), 1.48(3) Å) are of similar separation. Overall, there are 10 carbonyl ligands; one bridging the Os(3)−Rh(1) edge, two terminally bound to each Os(2), Os(3), and Rh(1) atom, and three being terminal on the Os(1) atom. The alkenyl proton on C(11) was located by a potential energy calculation. Hence, complex **6** obeys the EAN rule with 62 CVE in the five metal−metal bonds arranged in a butterfly structure.

The three heptanuclear cluster products $[N(PPh_3)_2][Os_6Rh(\mu\text{-}H)_2(CO)_{20}]$ (**2**), $[Os_6Rh(\mu\text{-}H)_7(\mu\text{-}CO)(CO)_{18}]$ (**3**), and $[Os_6Rh(\mu\text{-}H)_9(CO)_{18}]$ (**5**) have similar structures; therefore, we attempted to interconvert them by hydrogenation, protonation in acidic medium (addition of $HBF_4$ or $H_2SO_4$). and carbonylation. However, we observed no interconversion of **2**, **3**, and **5** in these reactions, as indicated by IR and $^1$H NMR spectroscopy.

## Experimental Section

All reactions and manipulations were carried out under an inert atmosphere using standard Schlenk techniques. Solvents were purified by standard procedures and freshly distilled prior to use. All chemicals, except where stated, were purchased commercially and used as received. The complexes $[N(PPh_3)_2][Os_3(\mu\text{-}H)(CO)_{11}]$,[24] $[Os_3(\mu\text{-}H)_2(CO)_{10}]$,[25] $[Rh(COD)_2][SbF_6]$,[26] and $[Rh(dppm)_2][BF_4]$[27] were prepared by literature methods. Infrared spectra were recorded on a Bio-Rad FTS-7 IR spectrometer, using 0.5 mm calcium fluoride solution cells, and proton NMR spectra at 25 °C on a Bruker DPX 300, using $CD_2Cl_2$ and referenced to $SiMe_4$ ($\delta$ 0 ppm), while $^{31}$P spectra were recorded on a Bruker DPX 500 NMR spectrometer, using $CDCl_3$ as solvent and 85% $H_3PO_4$ as reference. Mass spectra were recorded on a Finnigan MAT 95 instrument by the fast atom bombardment technique, using *m*-nitrobenzyl alcohol or α-thioglycerol as the matrix solvents. Microanalyses were performed by Butterworth Laboratories, Middlesex, U.K. Routine purification of products was carried out in air by thin-layer chromatography on plates coated with Merck Kieselgel 60 $GF_{254}$.

Author: Please give the city in the U.K. for the location of Butterworth Laboratories (above).

**Reaction of $[N(PPh_3)_2][Os_3(\mu\text{-}H)(CO)_{11}]$ with $[Rh(COD)_2][SbF_6]$.** A red solution of $[N(PPh_3)_2][Os_3(\mu\text{-}H)(CO)_{11}]$ (50 mg, 0.035 mmol) in $CH_2Cl_2$ (20 cm$^3$) was stirred with 1 equiv of $[Rh(COD)_2][SbF_6]$ (16 mg, 0.035 mmol) under dinitrogen gas. The color gradually turned to dark brown. Stirring was continued until all starting materials were consumed (TLC monitoring, 30 min). The solvent was removed in vacuo, and the residue was chromatographed on silica using *n*-hexane−$CH_2Cl_2$ (2:1, v/v) as eluent. Two bands were eluted. The first orange band yielded the known cluster $[Os_3Rh(\mu\text{-}H)_3(CO)_{10}(COD)]$ (**1**: $R_f$ 0.70; 8 mg, 0.008 mmol, 25%), as shown by IR, $^1$H NMR, and MS. The second green band gave $[N(PPh_3)_2][Os_6Rh(\mu\text{-}H)_2(CO)_{20}]$ (**2**: $R_f$ 0.3; 6 mg, 0.002 mmol, 12%). Anal. Found: C, 28.6; H, 1.5; N, 0.6. Calcd for $C_{56}H_{32}O_{20}NP_2Os_6Rh$ (**2**): C, 28.7; H, 1.4; N, 0.6.

**Synthesis of $[Os_6Rh(\mu\text{-}H)_7(\mu\text{-}CO)(CO)_{18}]$ (3).** A solution of $[Os_3(\mu\text{-}H)_2(CO)_{10}]$ (50 mg, 0.059 mmol) in $CHCl_3$ (30 cm$^3$)

---

[24] Abel, E. W.; Bennett, M. A.; Wilkinson, G. *J. Chem. Soc.* **1959**, 3178.

[25] Sappa, E.; Ville, M. *Inorg. Synth.* **1989**, *26*, 367.

[26] Adatia, T.; Curtis, H.; Johnson, B. F. G.; Lewis, J.; McPartlin, M.; Morris, J. *J. Chem. Soc., Dalton Trans.* **1994**, 3069.

[27] Sanger, A. R. *J. Chem. Soc., Dalton Trans.* **1977**, 120.

**Table 6. Crystallographic Data and Data Collection Parameters for Compounds 2, 3, 5, and 6**

| | **2** | **3** | **5** | **6** |
|---|---|---|---|---|
| empirical formula | $C_{56}H_{32}NO_{20}P_2Os_6Rh$ | $C_{19}H_7O_{19}Os_6Rh$ | $C_{18}H_9O_{18}Os_6Rh$ | $C_{38}H_{21}O_{10}Os_6Rh$ |
| $M_r$ | 2344.92 | 1783.36 | 1757.36 | 1311.08 |
| cryst dimens/mm | 0.17 × 0.21 × 0.22 | 0.21 × 0.21 × 0.23 | 0.12 × 0.12 × 0.23 | 0.18 × 0.21 × |
| cryst syst | monoclinic | monoclinic | triclinic | triclinic |
| space group | $C2/c$ (No. 15) | $P2_1/n$ (No. 14) | $P\bar{1}$ (No. 2) | $P\bar{1}$ (No. 2) |
| $a$/Å | 27.884(3) | 10.643(1) | 9.206(1) | 9.941(1) |
| $b$/Å | 18.235(1) | 18.929(2) | 9.709(1) | 10.675(1) |
| $c$/Å | 26.663(2) | 16.048(1) | 11.207(1) | 18.126(2) |
| $\alpha$/deg | 90 | 90 | 100.16(1) | 83.09(1) |
| $\beta$/deg | 112.09(2) | 97.17(1) | 105.14(1) | 85.44(1) |
| $\gamma$/deg | 90 | 90 | 117.55(2) | 68.91(1) |
| $U$/Å$^3$ | 12562(2) | 3207.8(5) | 803.9(3) | 1780.3(4) |
| $Z$ | 8 | 4 | 1 | 2 |
| $D_{calcd}$ /g cm$^{-3}$ | 2.480 | 3.692 | 3.630 | 2.446 |
| temp/K | 298 | 298 | 298 | 298 |
| $\mu$/cm$^{-1}$ | 124.58 | 242.29 | 241.64 | 111.78 |
| $F$(000) | 8528 | 3096 | 762 | 1204 |
| max 2$\theta$/deg | 51.2 | 51.1 | 51.0 | 51.1 |
| no. of unique rflns collected | 10 452 | 6051 | 2626 | 5505 |
| no. of obsd rflns ($I > 3.00\sigma(I)$) | 5002 | 4271 | 1920 | 3361 |
| $\rho$ in weighting scheme[a] | 0.020 | 0.023 | 0.020 | 0.021 |
| $R$ indices (obsd data) | $R = 0.044$<br>$R' = 0.046$ | $R = 0.032$<br>$R' = 0.038$ | $R = 0.063$<br>$R' = 0.081$ | $R = 0.052$<br>$R' = 0.059$ |
| goodness of fit | 1.39 | 1.14 | 1.61 | 1.66 |
| largest $\Delta/\sigma$ | 0.03 | 0.09 | 0.02 | 0.01 |
| no. of params | 393 | 406 | 106 | 229 |
| residual extrema in final diff map (close to Os)/e Å$^{-3}$ | +1.29 to −1.56 | +1.17 to −1.80 | +1.66 to −3.60 | +1.45 to −2.24 |

[a] $w = [\sigma_c^2(F_o) + \rho^2/4(F_o^2)]^{-1}$.

was stirred with $[Rh(dppm)_2][BF_4]$ (57 mg, 0.059 mmol) under a dinitrogen atmosphere. The initial dark red solution changed to orange after reflux for 15 h. The solvent was removed in vacuo, and the products were separated by TLC using *n*-hexane−$CH_2Cl_2$ (3:1, v/v). A band was then eluted, identified as $[Os_6Rh(\mu\text{-}H)_7(\mu\text{-}CO)(CO)_{18}]$ (**3**: $R_f$ 0.65; 30 mg, 0.017 mmol, 30%) Anal. Found: C, 12.6; H. 0.5. Calcd for $C_{19}H_7O_{19}Os_6Rh$ (**3**): C, 12.8; H, 0.4.

**Reactions of 1 with Carbon Monoxide.** Compound **1** (20 mg, 0.019 mmol) was redissolved in $CH_2Cl_2$ (10 cm$^3$). CO gas was bubbled into the solution at room temperature, and the mixture turned yellow gradually. It was then stirred for 30 min beyond the time all the starting materials were consumed. After the volume was reduced, the filtrate was separated by preparative TLC on silica with an eluent of *n*-hexane−$CH_2Cl_2$ (3:1, v/v). The cluster product $[Os_3Rh(\mu\text{-}H)_3(CO)_{12}]$ (**4**) was isolated with an $R_f$ value of 0.55 (8 mg, 0.008 mmol, 42%).

**Reaction of 1 with Hydrogen.** Hydrogen gas was bubbled through a solution of cluster **1** (30 mg, 0.028 mmol) in $CH_2Cl_2$ for 15 h. The solvent was then removed under reduced pressure and the residue separated by preparative TLC plates using *n*-hexane−$CH_2Cl_2$ (1:1, v/v) as eluent. Two consecutive bands were eluted, namely the unreacted cluster **1** and a red band of **5** ($R_f$ 0.6; 5 mg, 0.003 mmol, 20%). Other products decomposed on plates. Anal. Found: C, 12.2; H, 0.5. Calcd for $C_{18}H_9O_{18}Os_6Rh$ (**5**): C, 12.3; H, 0.5.

**Reaction of 1 with [PhC$_2$Ph].** The compounds $[PhC_2Ph]$ (5.0 mg, 0.028 mmol) and $[Os_3Rh(\mu\text{-}H)_3(CO)_{10}(COD)]$ (**1**; 30 mg, 0.028 mmol) were mixed in $CHCl_3$ (20 cm$^3$) under nitrogen. Refluxing for 3 h resulted in a color change from orange to reddish brown. The solution was reduced in vacuo, and the residue was separated by TLC using *n*-hexane−$CH_2Cl_2$ (7:1, v/v) to afford the major product, **6** ($R_f$ 0.4; 3 mg, 0.002 mmol, 8%). Anal. Found: C, 34.8; H, 1.5. Calcd for $C_{38}H_{21}O_{10}Os_3Rh$ (**6**): C, 34.8; H, 1.6.

**Reaction of [N(PPh$_3$)$_2$][Os$_3$($\mu$-H)(CO)$_{11}$] with [Os$_3$Rh($\mu$-H)$_3$(CO)$_{12}$] (4).** A solution of $[N(PPh_3)_2][Os_3(\mu\text{-}H)(CO)_{11}]$ (42 mg, 0.03 mmol) and $[Os_3Rh(\mu\text{-}H)_3(CO)_{12}]$ (**4**; 30 mg, 0.03 mmol) in $CH_2Cl_2$ was stirred at room temperature under nitrogen for 5 min. An immediate color change to green was observed. The solution was concentrated in vacuo, and the residue was chromatographed by *n*-hexane−$CH_2Cl_2$ (1:1, v/v). The green eluant was identified as $[N(PPh_3)_2][Os_6Rh(\mu\text{-}H)_2(CO)_{20}]$ (**2**: $R_f$ 0.3; 24 mg, 0.009 mmol, 32%).

**Crystallography.** Crystals suitable for X-ray analyses were glued on glass fibers with epoxy resin and mounted on a MAR research image plate scanner equipped with graphite-monochromated Mo K$\alpha$ radiation ($\lambda$ = 0.710 73 Å) for unit-cell determination and data collection. Pertinent crystallographic data and other experimental details are summarized in Table 6. Data were collected using the $\omega$-scan technique with 65 3° frames and an exposure time of 5 min per frame. The diffracted intensities were corrected for Lorentz and polarization effects. An approximation to absorption correction by interimage scaling was made for all the complexes. Scattering factors were taken from ref 28a, and anomalous dispersion effects[28b] were included in $F_c$. The structures were solved by direct methods (SIR 88)[29] and expanded by difference Fourier techniques. The structure was refined on $F$ by full-matrix least-squares analysis with Os and Rh atoms refined anisotropically. The positions of hydride ligands in **2**, **3**, and **6** were estimated by potential energy calculations.[30] The hydrogen atoms in the organic moieties were placed in their idealized positions (C−H, 0.95 Å). All the hydrogen atoms were included in the structure factors, but the parameters were not refined. In the crystal structure of **2**, there are two independent half-molecules with two independent Rh atoms and two N atoms of $[N(PPh_3)_2]^+$ cation occupy the $C_2$ symmetry axis. Only one of the Rh−Os mixed-metal cluster anions is shown in Figure 1. In the crystal structure of **5**, the Rh atom resides on the center of inversion in space group $P\bar{1}$ (No. 2). It is believed that the molecule does not contain a center of symmetry, but pseudo-symmetry arises from a random distribution of two orientations of the cluster.

---

[28] (a) Cromer, D. T.; Waber, J. T. *International Tables for X-ray Crystallography;* Kynoch Press: Birmingham, U.K., 1974; Vol. 4, Table 2.2B. (b) *Ibid*., Table 2.3.1.

[29] Burla, M. C.; Camalli, M.; Cascarnao, G.; Giacovazzo, C.; Polidor, G.; Spagna, R.; Viterbo, D. SIR 88. *J. Appl. Crystallogr.* **1989**, *22*, 389.

[30] Orpen, A. G. *J. Chem. Soc., Dalton Trans.* **1980**, 2509.

Calculations were performed on a Silicon Graphics computer, using the teXsan program package.[31]

Atomic coordinates, thermal parameters, and bond lengths and angles have been deposited at the Cambridge Crystallographic Data Center (CCDC).

**Acknowledgment.** W.-T.W. gratefully acknowledges financial support from the Croucher Foundation and the University of Hong Kong (AOD Grant). Miss Hung Yeuk-Wah is thanked for technical support in this work.

**Supporting Information Available:** Full details of the crystallographic analyses, including tables of crystallographic data, atomic coordinates, bond lengths, bond angles, hydrogen coordinates, and anisotropic displacement parameters for complexes **2**, **3**, **5,** and **6**. This material is available free of charge via the Internet at http://pubs.acs.org.

OM9900925

---

[31] teXsan, Crystal Structure Analysis Package; Molecular Structure Corp., Houston, TX, 1985 and 1992.